Japanese Journal of Radiology (2020) 38:463–471
https://doi.org/10.1007/s11604-020-00931-7

ORIGINAL ARTICLE

Chronic inflammation-related radiological findings of gallbladder adenomyomatosis

Hyeon Jin Lee[1] · Woo-Suk Chung[1] · Ji Youn Kim[1] · Ji hae An[1] · Shinyoung Park[2]

Received: 19 November 2019 / Accepted: 10 February 2020 / Published online: 18 February 2020

Abstract

Purpose This study aimed to assess radiological findings of adenomyomatosis advancing to chronic inflammation to differentiate between adenomyomatosis with and without chronic inflammation.

Materials and methods We retrospectively identified 79 patients with pathologically proven adenomyomatosis without ($n=10$) or with chronic inflammation ($n=69$), who underwent computed tomography (CT) and magnetic resonance imaging (MRI) followed by surgery. MRI analysis included evaluation of GB wall-thickening type, presence and location of intramural cysts, and presence of stones. CT analysis included GB wall-thickening type only. Multivariate logistic regression analysis was used to identify the image-based findings of adenomyomatosis associated with chronic inflammation.

Results On univariate analysis, MRI-based GB wall-thickening type and presence of stones, and CT-based GB wall-thickening type were significantly different between adenomyomatosis with and without chronic inflammation. On multivariate analysis, only the absence of stones was identified as a significant predictor of adenomyomatosis without chronic inflammation (odds ratio 5.58; 95% confidence interval 1.20–26.01; $p=0.029$). There was no significant difference in other MRI- and CT-based findings between adenomyomatosis with and without chronic inflammation.

Conclusion In patients with adenomyomatosis, the presence of stones was independently associated with chronic inflammation.

Keywords Adenomyomatosis · Computed tomography · Gallbladder · Inflammation · Magnetic resonance imaging

Introduction

Adenomyomatosis (ADM) of the gallbladder (GB) is a benign, acquired pathology that is defined as the proliferation of the mucosal epithelium and hypertrophy of the muscularis mucosae, with outpouching of the mucosa into or through the thickened muscular layer, forming so-called Rockitansky–Aschoff sinus [1, 2]. ADM is classified into three macroscopic types: fundal, segmental, and diffuse [3]. ADM is not considered a premalignant lesion. ADM theoretically requires no specific treatment, except when symptomatic, with or without GB stones [3]. However, the differentiation of this condition from GB cancer is still necessary, because of the similarity in the appearance between ADM and GB cancer [4–6]. Segmental type ADM reportedly has a higher risk of developing into GB cancer, especially when occurring in the fundal region of the GB in elderly patients [7]. Radiological follow-up or cholecystectomy might be considered in patients with the segmental type of ADM [3].

Current data do not indicate ADM as a risk factor for malignant degeneration. However, both ADM and GB cancer have a common background of chronic inflammation. GB cancer is associated with chronic inflammation due to GB stones. Motility disorders of the GB and chronic GB inflammation have been suspected to be associated with the pathogenesis of ADM [3]. ADM also appears to play a role in the formation of GB stones [8, 9]. It is possible that chronic inflammation secondary to ADM may lead to dysplastic changes and cancer. However, to the best of our knowledge, no previous reports have assessed the factors related to chronic inflammation in ADM to date.

✉ Woo-Suk Chung
radcws@gmail.com

[1] Department of Diagnostic Radiology, Konyang University Hospital, Konyang University College of Medicine, 158 Gwanjeodong-ro, Seo-gu, Daejeon 35365, South Korea

[2] Department of Pathology, Daejeon Sun Hospital, Daejeon, South Korea

Therefore, the purpose of this study was to assess radiological findings of ADM associated with chronic inflammation that may allow prediction of ADM without chronic inflammation to that with chronic inflammation.

Materials and methods

Patients

Between January 2007 and November 2018, among 3269 patient who underwent cholecystectomy, 184 consecutive patients with pathologically proven ADM were identified through a review of our institutional pathological and radiological database. The inclusion criteria were shown as follows: (a) patients with surgically proven ADM, (b) who underwent computed tomography (CT) and magnetic resonance imaging (MRI) examination before surgery. One hundred-five patients were excluded from the analysis because (a) they did not undergo MRI and CT within three months before surgery ($n=100$), (b) had suboptimal image quality on MRI ($n=4$), or (c) had severe acute inflammation ($n=1$). Finally, 79 patients (mean age 54.0 ± 14.3 years; age range 17–82 years; male:female ratio 43:36) were included in our study. This study population comprised 10 patients with ADM without chronic inflammation (mean age 53.9 ± 11.5 years; age range 38–77 years; male:female ratio 8:2) and 69 patients with ADM with chronic inflammation (mean age 54 ± 14.7 years; age range 17–82 years; male:female ratio 35:34). These 79 patients all had histopathologically confirmed diagnosis by cholecystectomy. One of the 10 patients with ADM without chronic inflammation had cholesterol polyps and 2 of 69 patients with ADM with chronic inflammation respectively had a type I choledochal cyst and GB cancer arising from ADM. The mean interval between imaging studies and cholecystectomy was 8.7 ± 11.4 days (range 1–60 days) for MRI and 16.6 ± 19.1 days (range 1–90 days) for CT.

Our institutional review board approved this study, and the need to obtain informed patient consent was waived due to the retrospective nature of the study.

MRI and CT techniques

MRI was performed with two 3-T units (Achieva 3.0 T [$n=49$], Philips Medical Systems, Best, The Netherlands; Ingenia 3.0 T [$n=30$], Philips Medical Systems) using a torso phased-array coil (Achieva 3.0 T, 16 channels XL torso coil; Ingenia 3.0 T, 32 channels dS torso coil) covering the abdomen. Patients were asked to fast for a minimum of 6 h. Contrast agents and antispasmodic agents were not used. At baseline, MR images were obtained using a T1-weighted turbo field-echo in-phase (repetition time [TR]/echo time [TE] 144.6/4.6 [Achieva 3.0 T, A] or 4.7/2.3 [Ingenia 3.0 T, I]; flip angle, 55 degrees [A] or 10 degrees [I]; echo-train length, 3 [A] or 213 [I]; matrix size, 168×177 [A] or 176×176 [I]; slice thickness, 5 mm) and opposed-phased (TR/TE 144.6/3.5 [A] or 4.7/1.2 [I]; flip angle, 55 degrees [A] or 10 degrees [I]; echo-train length, 3 [A] or 213 [I]; matrix size, 168×177 [A] or 176×176 [I]; slice thickness, 5 mm) sequence. Additionally, a breath-hold multishot T2-weighted sequence (TR/TE 2572.2/80 [A] or 1749.1/80 [I]; flip angle, 90 degrees; echo-train length, 25 [A] or 16 [I]; matrix size, 292×250 [A] or 256×192 [I]; slice thickness, 5 mm), and a respiratory-triggered single-shot T2-weighted (TR/TE 778.7/80 [A] or 1084/80 [I]; flip angle, 90 degrees; echo-train length, 57 [A] or 78 [I]; matrix size, 296×216 [A] or 320×254 [I]; slice thickness, 5 mm), as well as coronal heavily T2-weighted (TR/TE 1398.4/140 [A] or 899/160 [I]; flip angle, 90 degrees; echo-train length, 117 [A] or 93 [I]; matrix size, 356×303 [A] or 268×264 [I]; slice thickness, 3 mm) sequences were used. The field of view was 350 mm and was adjusted according to the patient size. Two methods of magnetic resonance cholangiopancreatography (MRCP) were used to evaluate ADM. Sequence parameters of MRCP were chosen according to the protocols optimized by the vendor. First, a breath-hold single-section two-dimensional single-shot turbo spin-echo MRCP sequence (TR/TE 5890×930 [A] or 6176.6/920 [I]; flip angle, 90 degrees; echo-train length, 256 [A] or 255 [I]; matrix size, 256×256 [A] or 320×255 [I]; slab thickness, 50 mm) in the coronal plane was performed. Subsequently, a navigator-triggered three-dimensional MRCP turbo spin-echo sequence (TR/TE 1957.2/600 [A] or 285.4/110.1 [I]; flip angle, 90 degrees; echo-train length, 112; matrix size, 256×256; slab thickness, 2 mm) was performed in the coronal plane. Maximum intensity projections in an analogous orientation of navigator-triggered three-dimensional MRCP turbo spin-echo sequences were generated from the MR console using the manufacturer's imaging reconstruction process (Advance Viewer; Philips Medical Systems).

CT imaging was performed with three scanners; a 16-channel MDCT scanner (Mx8000 IDT 16 [$n=12$], Philips Medical Systems, Andover, MA, USA), a 64-channel MDCT scanner (Aquilion [$n=37$], Toshiba Medical Systems Corp, Tokyo, Japan) and a 128-channel MDCT (Somatom Definition Flash [$n=30$], Siemens Healthcare, Forchheim, Germany). The following scanning parameters were used for the 16-MDCT scanner: 16×1.5 mm collimation, a pitch of 1 and a rotation time of 0.75 s. The parameters for the 64-MDCT scanner were: 64×0.5 mm collimation, a pitch of 0.813 and a rotation time of 0.5 s. The parameters for the 128-MDCT were: a 128×0.6 mm collimation, a pitch of 0.8 and a rotation time of 0.5 s. The kilovoltage and effective tube current–time charge were between 100 and 120 kV and between 100 and

250 mAs, respectively. Before CT scanning, each patient had fasted for over 6 h, and received a 2 mL/kg intravenous dose (total volume < 150 mL; 3 mL/s) of nonionic contrast material through an 18-gauge angiographic catheter inserted into a forearm vein, using an automatic power injector (Stellant D, Medrad, Pittsburgh, PA, USA). After obtaining unenhanced CT images, portal venous phase images were acquired 60–70 s after administration of contrast medium. CT scans were obtained in the supine position, and the scanning field ranged from the diaphragmatic dome to the anal verge. All examinations were performed during deep inspiration. Axial CT images were reconstructed with a 3–5 mm section thickness and a 3–5 mm reconstruction interval for clinical interpretation. In addition to the axial images, coronal MPR images were reconstructed with a 3–5 mm section thickness at a 3–5 mm interval.

Image analysis

Two radiologists (W.S.C. and H.J.L., with 16 and 3 years of clinical experience in interpreting MRI and CT images, respectively) retrospectively reviewed the MRI- and CT-based findings in consensus. They knew that the patients had been referred for evaluation of ADM but had no knowledge of the final radiologic or pathologic findings. The images were presented to the reviewers in a random sequence. All MRI and CT scans were reviewed on a PACS workstation (INFINITT PACS M6, Infinitt Healthcare Co., Seoul, Korea).

The following parameters were investigated on MRI: GB wall-thickening type, presence of intramural cysts, location of intramural cysts, and presence of stones. We classified ADM according to the gross features of the specimens [3]. First, the fundal type was defined as a hemispheric, elevated lesion with a central dimple located at the tip of the GB (Fig. 1). Second, the segmental type was defined as an annular or segmental wall-thickening that divided the GB

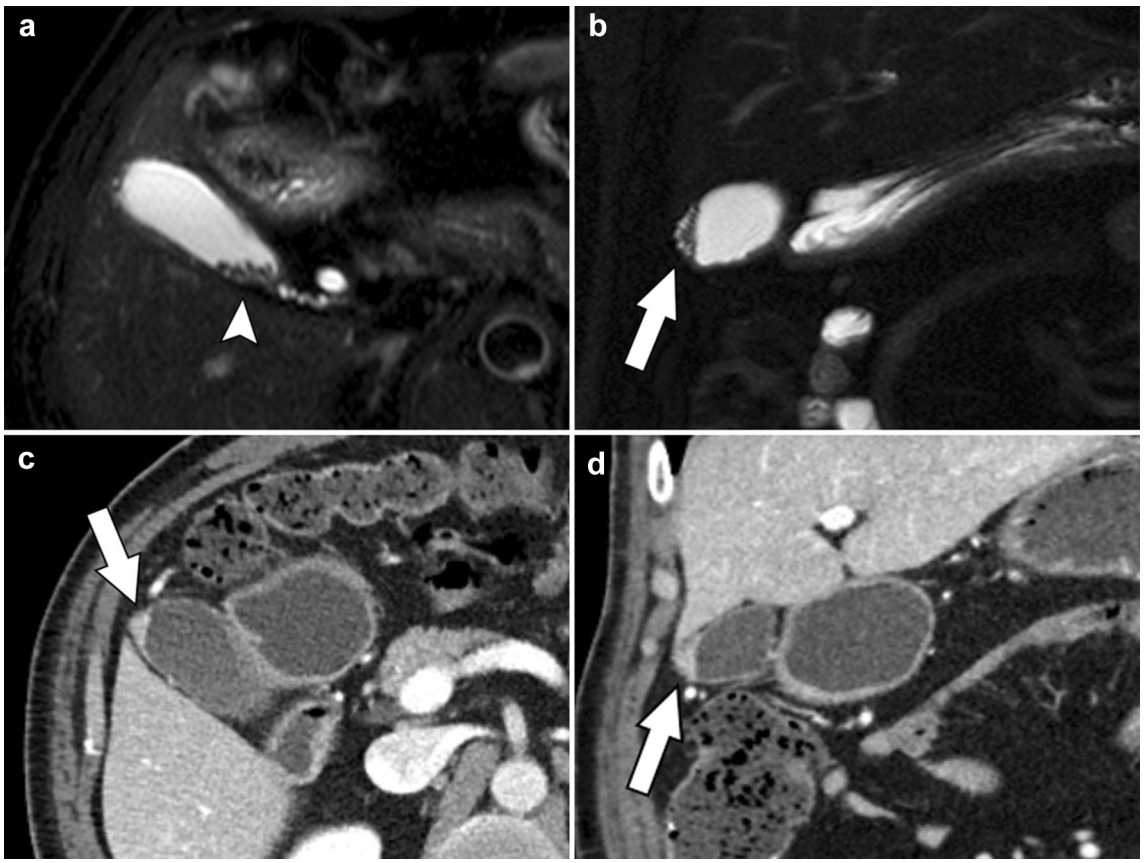

Fig. 1 Fundal adenomyomatosis of the gallbladder (GB) in a 60-year-old man. Magnetic resonance (MR) images with breath-hold multishot T2-weighted sequence (**a**) and coronal heavily T2-weighted sequence (**b**) show a hemispheric, elevated lesion with intramural cysts located at the tip of the GB (arrow). MR images demonstrate multiple small GB stones (arrowhead). Axial (**c**) and coronal (**d**) computed tomography images during the portal venous phase show fundal abnormality with enhancing epithelium and without intramural low attenuations (arrow). Fundal adenomyomatosis with chronic inflammation was pathologically confirmed

lumen into separate, interconnected compartments (Fig. 2). Third, the diffuse type was defined as wall-thickening present throughout the entire GB. MR GB wall-thickening was classified as the fundal type or combined type (segmental type and diffuse type). Intramural cysts were defined as a Rokitansky–Aschoff sinus filled with bile within a thickened GB wall that manifested as markedly hyperintense spots on the T2-weighted MR image. Both the presence and location of intramural cysts were evaluated. If intramural cysts were present, the location of the intramural cysts was classified according to GB anatomy (fundus, body, and neck). If intramural cysts were present in the fundus alone, they were classified as "fundus"; alternatively, they were classified as "other". The presence of stones was also analyzed. GB stones were defined as stones within the lumen of the GB and did not include intramural small concretions within Rokitansky–Aschoff sinuses.

CT-based GB wall-thickening was reviewed in each contrast-enhanced CT image. GB wall-thickening was evaluated according to thickened wall enhancement as compared to the adjacent normal GB wall. Fundal type of CT GB wall-thickening was defined as a hemispheric, elevated or thickened wall enhancement, with or without intramural low attenuation, located at the tip of the GB. Combined type was defined as segmental and diffuse-type CT GB wall-thickening according to thickened wall enhancement, with or without intramural low attenuation.

Histologic examination

Seventy-nine patients had a diagnosis of ADM that was histopathologically confirmed after cholecystectomy. The histopathologic findings in surgical specimens from all patients were retrospectively reviewed by one pathologist. The type of ADM was pathologically classified as fundal or combined type. Chronic inflammation was pathologically defined as the existence of acute inflammation, chronic inflammation, and chronic cholecystitis. Cholelithiasis was

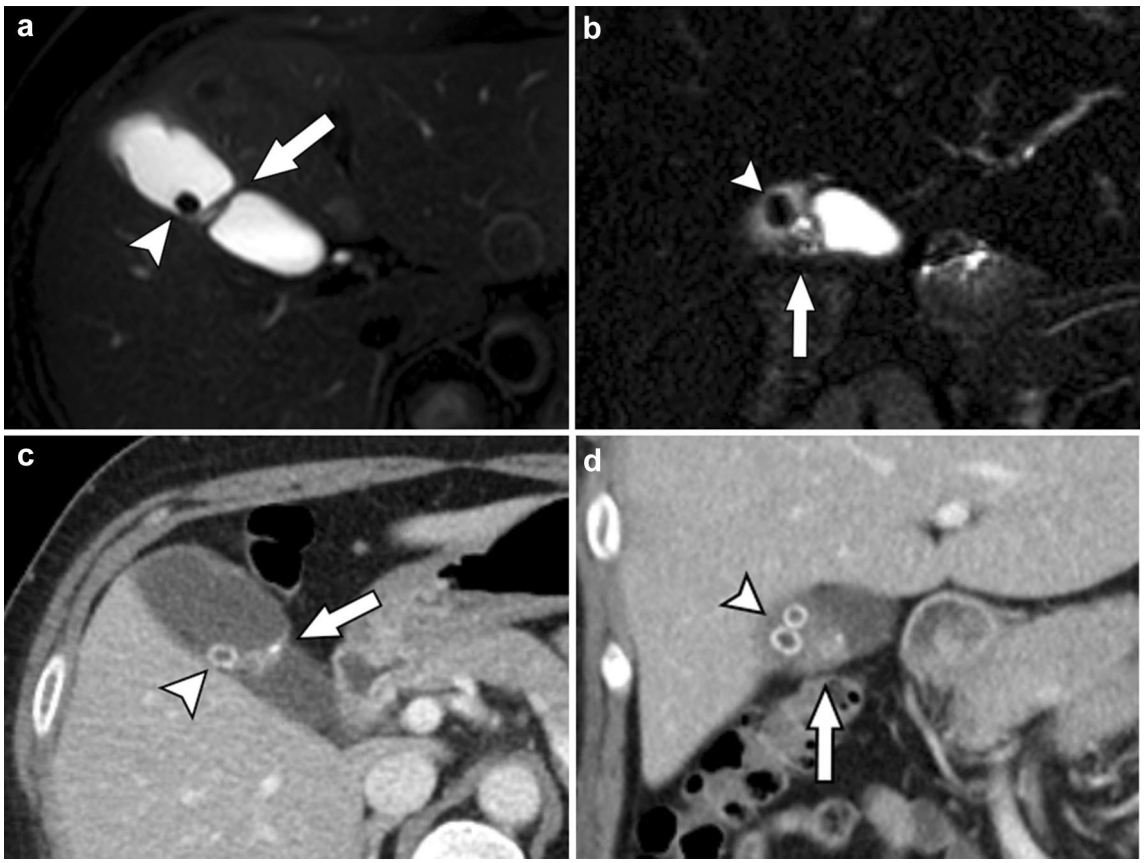

Fig. 2 Segmental adenomyomatosis of the gallbladder (GB) in a 43-year-old woman. Magnetic resonance (MR) images with a breath-hold multishot T2-weighted sequence (**a**) and coronal heavily T2-weighted sequence (**b**) show segmental thickening with intramural cysts in the body of the GB (arrow). MR images demonstrate GB stones (arrowhead). Axial (**c**) and coronal (**d**) computed tomography (CT) images during portal venous phase show segmental wall thickening with contrast enhancement and without intramural low attenuations at the GB body (arrow). CT images also demonstrate GB stones (arrowhead). Segmental adenomyomatosis with chronic inflammation was pathologically confirmed

also pathologically reviewed for evaluation of GB stones identified by MRI.

Statistical analysis

All of the statistical analyses were performed using R version 3.5.2. Continuous variables were presented as mean and standard deviation (SD) and compared using the unpaired *t* test. Categorical variables were compared using Fisher's exact test. Univariate and multivariate analyses were performed to determine the variables that were associated with ADM without chronic inflammation. The diagnostic performance of significant radiological findings in terms of the differentiation between ADM without chronic inflammation and ADM with chronic inflammation was performed using receiver operating characteristic (ROC) curve analysis. To determine the diagnostic accuracy, the area under the ROC curve (Az) value was evaluated. The Az values acquired from the ROC curves were statistically compared using the paired *Z* test. Sensitivity, specificity, positive-predictive value (PPV), negative-predictive value (NPV), and accuracy of parameters for the diagnosis of ADM without chronic inflammation were assessed using the McNemar test with Bonferroni correction. p values of <0.05 were considered to indicate statistical significance.

Results

The prevalence of ADM in cholecystectomized patients was 5.6% (184/3269). The prevalence of GB stones was 69.6% (55/79) in patients with ADM, 56.7% (17/30) in patients with fundal type of MR GB wall-thickening, and 77.6% (38/49) in patients with combined type of MR GB wall-thickening. All GB stones detected on MRI were pathologically confirmed as cholelithiasis. The mean size of GB stones in ADM with and without chronic inflammation was 0.69 ± 0.49 cm and 0.5 ± 0.17 cm, respectively ($p = 0.189$). Pathologic diagnosis of type of ADM was consistent with MR GB wall-thickening type.

The results of univariate and multivariate analyses of clinical and radiological findings related to chronic inflammation in patients with ADM are shown in Tables 1 and 2, respectively. Chronic inflammation in the ADM correlated with MR GB wall-thickening, GB stones, and CT GB wall-thickening in univariate analysis ($p = 0.031$, 0.007, and 0.016, respectively), whereas multivariate analysis identified only the absence of GB stones as a factor independently associated with ADM without chronic inflammation (odds ratio [OR], 5.58; 95% confidence interval [CI], 1.20–26.02; $p = 0.029$) (Fig. 3, 4). No significant difference was noted between the groups in terms of the presence of intramural cysts. The location of intramural cysts also showed no significant difference for differential diagnosis of ADM without chronic inflammation and ADM with chronic inflammation.

Table 1 Comparison of clinical and radiological findings in adenomyomatosis without and with chronic inflammation

	Chronic inflammation		*p* value
	Negative	Positive	
Age (years, mean ± SD)	53.9 ± 11.5	54 ± 14.7	0.265
Sex			
Male	8	35	0.079
Female	2	34	
MR GB wall-thickening			
Fundal type	7	23	0.031
Combined type	3	46	
Intramural cysts			
Absent	2	13	0.608
Present	8	56	
GB stone			
Absent	7	17	0.007
Present	3	52	
CT GB wall-thickening			
Fundal type	7	20	0.016
Combined type	3	49	

GB gall bladder, *MR* magnetic resonance, *CT* computed tomography

The Az values and ROC curves of MR GB wall-thickening, GB stones, and CT GB wall-thickening, which showed significant differences in the univariate analysis for differential diagnosis of ADM without chronic inflammation and ADM with chronic inflammation, are shown in Table 3 and Fig. 5. GB stones showed the highest Az value. However, no significant difference was found in the Az values among the three variables ($p > 0.05$). The sensitivity, specificity, PPV, NPV, and accuracy of the three variables are shown in Table 3. GB stones showed the highest specificity, PPV, and NPV; however, the sensitivity, specificity, PPV, NPV, and accuracy of these three variables did not differ statistically significantly ($p > 0.05$).

Discussion

In this study, we investigated whether radiological findings could be used to distinguish between ADM with and without inflammation. We found that the presence of stones in the GB on MRI was associated with chronic inflammation in patients with ADM.

The prevalence of GB stones in cholecystectomized patients with ADM is high, ranging from 51.9 to 78% [10]. Earlier detection of GB stones in patients with segmental ADM also suggests that segmental ADM creates

Table 2 Multivariate analysis of associated factors for chronic inflammation in adenomyomatosis

	Adenomyomatosis without chronic inflammation vs with chronic inflammation			
	p value	Odds ratio	95% confidence interval	
			Lower boundary	Upper boundary
MR GB wall-thickening				
Fundal type	0.936	1.12	0.07	16.83
Combined type		1		
Intramural cysts				
Absent	0.993	1.01	0.15	6.59
Present		1		
GB stone				
Absent	0.029	5.58	1.20	26.01
Present		1		
CT GB wall-thickening				
Fundal type	0.313	3.98	0.27	58.18
Combined type		1		

GB gall bladder, *MR* magnetic resonance, *CT* computed tomography

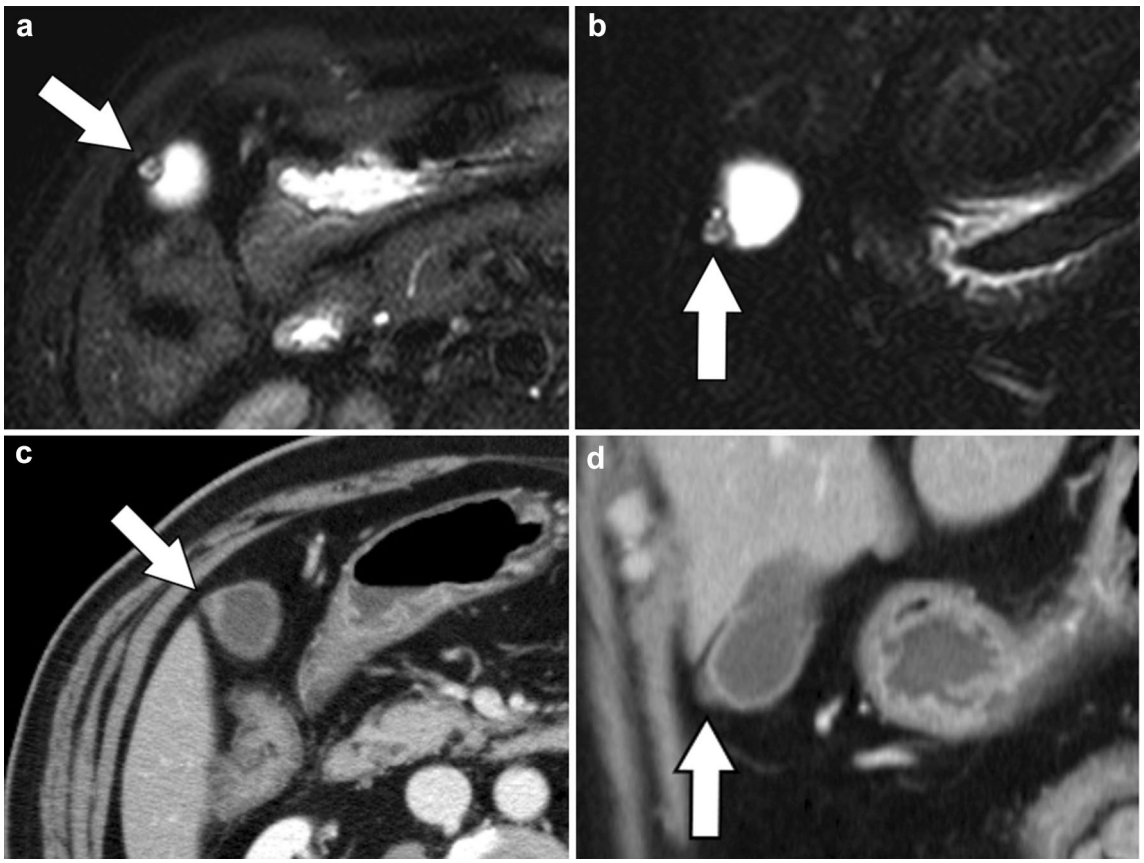

Fig. 3 Fundal adenomyomatosis of the gallbladder (GB) in a 53-year-old male. Magnetic resonance (MR) images with breath-hold multishot T2-weighted sequence (**a**) and coronal heavily T2-weighted sequence (**b**) show a hemispheric elevated lesion with intramural cysts located at the tip of the GB (arrow). MR images demonstrate no GB stone. Axial (**c**) and coronal (**d**) computed tomography (CT) images during the portal venous phase show fundal abnormality with enhancing epithelium and intramural low attenuations (arrow). Fundal adenomyomatosis without chronic inflammation was pathologically confirmed

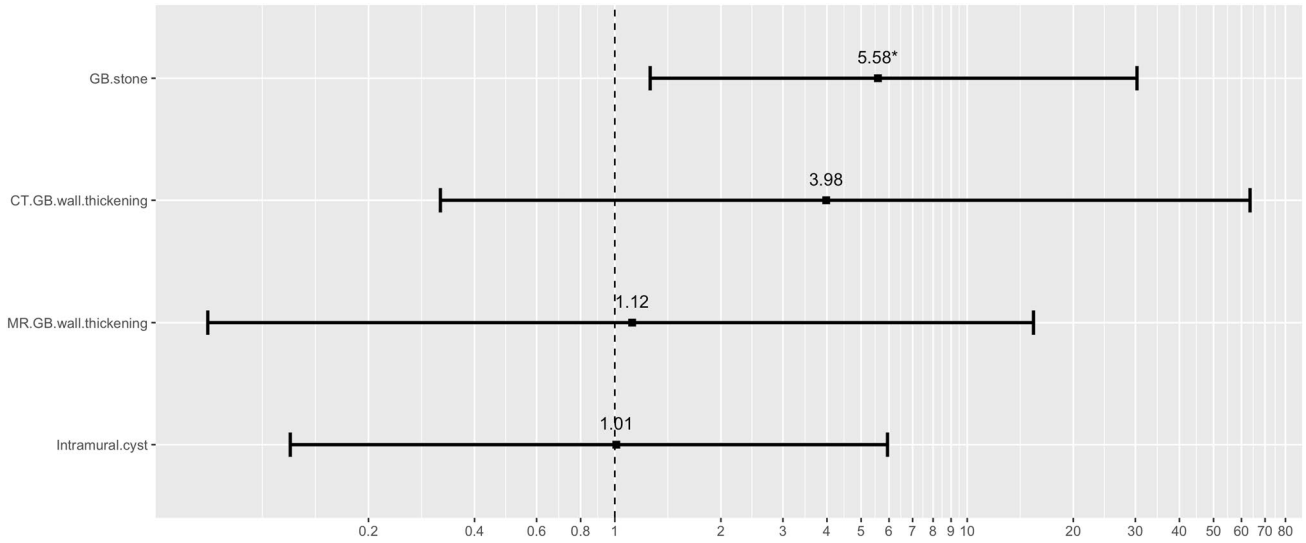

Fig. 4 Risk of chronic inflammation based on the radiological findings of adenomyomatosis. Odds ratio values with 95% confidence interval values for four radiological findings are plotted

Table 3 Diagnostic accuracy of significant variables in differentiating adenomyomatosis without chronic inflammation from that with chronic inflammation on univariate analysis

Variables	AUC	Sensitivity (%)	Specificity (%)	PPV (%)	NPV (%)	Accuracy (%)
MR GB wall-thickening	0.683 (0.524–0.843)	70.0 (34.8–93.3)	66.7 (54.3–77.6)	23.3 (9.9–42.3)	93.9 (83.1–98.7)	67.1 (55.6–77.3)
GB stone	0.727 (0.569–0.885)	70.0 (34.8–93.3)	75.4 (63.5–84.9)	29.2 (12.6–51.1)	94.5 (84.9–98.9)	74.7 (63.6–83.8)
CT GB wall-thickening	0.705 (0.546–0.864)	70.0 (34.8–93.3)	71.0 (58.8–81.3)	25.9 (11.1–46.3)	94.2 (84.1–98.8)	70.9 (59.6–80.1)

Data in parentheses are the 95% CI

GB gall bladder, *MR* magnetic resonance, *CT* computed tomography, *AUC* area under the curve, *PPV* positive-predictive value, *NPV* negative-predictive value

a predisposition to GB stone formation; additionally, the prevalence of GB stones was significantly higher in patients with segmental ADM than in those without ADM, while the prevalence of GB stones in patients with fundal or diffuse ADM and those without ADM was comparable in a previous study [9]. In our study, the prevalence of GB stones was 69.6% in patients with ADM, and more specifically, 56.7% in patients with fundal type of MR GB wall-thickening and 77.6% in patients with combined type of MR GB wall-thickening. The biliary stasis in the fundal compartment of segmental ADM may be responsible for the higher prevalence of GB stones in segmental than in fundal and diffuse ADM. Traditionally, ADM has not been regarded as having malignant potential, although GB cancer is associated with chronic inflammation caused by GB stones [11]. In our univariate analysis, MR GB wall-thickening, GB stones, and CT GB wall-thickening were significant factors for chronic inflammation. However, GB stones were the only significant factor identified in multivariate analysis, indicating that GB stones, but not the type of GB wall-thickening, are significantly associated with chronic inflammation.

Segmental ADM has a higher risk of developing into GB cancer, particularly in the fundal region of elderly patients [9]. In our study, one case with GB stones and combined type of MR GB wall-thickening had a carcinoma that arose from ADM. However, most investigators believe that development of carcinoma is related to the presence of stones, chronic inflammation, and metaplastic changes, rather than to ADM per se. Thus, ADM is not considered a premalignant lesion [6].

Although the pathogenesis of ADM has not been conclusively established, two hypothetical causes have been proposed. One is that it is a consequence of motility disorders of the GB and the other is that it is due to chronic inflammation. Bile stasis due to motility disorders of the GB may cause GB stones. Some studies have reported the association between ADM and anomalous pancreaticobiliary ductal union [12, 13]. This pancreaticobiliary maljunction may cause chronic inflammation due to chronic reflux of pancreatic fluid,

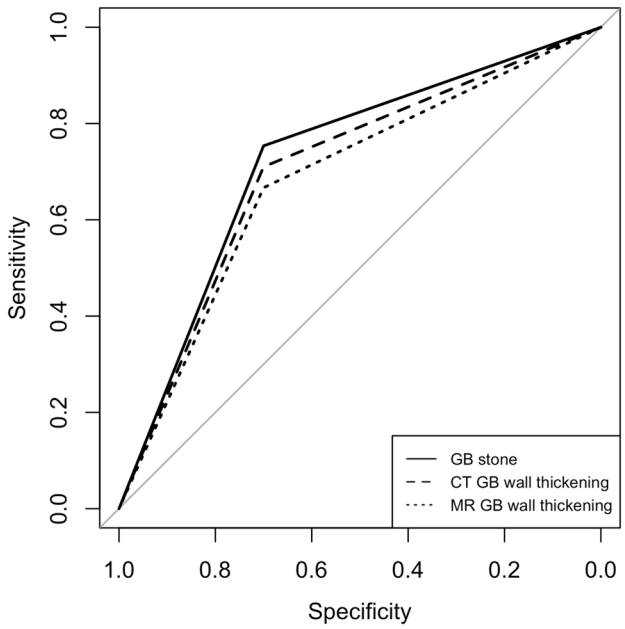

Fig. 5 Receiver operating characteristic curve for diagnostic performance of radiological findings. Receiver operating characteristic curves for diagnostic performance of radiological findings for differentiation of adenomyomatosis without chronic inflammation from that with chronic inflammation

leading to carcinogenesis through hyperplasia or intestinal metaplasia. In addition to the development of ADM, chronic inflammation may result from ADM. Complications of GB stones include cholecystitis, GB perforation, abscess formation, biliary obstruction, pancreatitis, and fistulation into the gastrointestinal tract. Chronic inflammation is a potent biliary carcinogen [14]. GB stones and chronic inflammation secondary to ADM may lead to dysplasia and cancer [15]. The present study showed the association between GB stones and chronic inflammation in patients with ADM.

The best imaging examination for ADM is MR cholangiography, which specifies the location of ADM. MRI readily demonstrates GB wall-thickening and reveals Rokitansky–Aschoff sinus as intramural lesions, which are hyperintense on T2-weighted images and hypointense on T1-weighted images [16]. The MRI protocol of this study did not include contrast enhancement. The type of GB wall-thickening was categorized on MRI based on intramural cysts of the thickened GB wall; enhancement was only used in CT. Abnormal GB wall-thickening and enhancement are common but nonspecific CT features of ADM. Rokitansky–Aschoff sinus of sufficient size can be visualized on CT as a rosary sign. Where Rokitansky–Aschoff sinuses are not visible; the thickening of the GB wall and enhancement pattern are relatively nonspecific, making it difficult to distinguish it from other conditions, including GB cancer [11], and indeed ADM and chronic cholecystitis are common diseases involving the GB that are sometimes hard to distinguish [17]. Therefore, the type of GB wall-thickening was classified as a fundal type and a combined type, due to the difficulty of distinguishing the segmental type and diffuse type, and to simplify assessment. In a univariate study, although both MR GB wall-thickening and CT GB wall-thickening were significant factors for chronic inflammation, the *p* value of CT GB wall thickening, when using contrast enhancement, was smaller than that of MR GB wall-thickening.

ADM is mainly an asymptomatic disease. The main treatment of symptomatic ADM with or without GB stone is laparoscopic cholecystectomy [18]. However, in addition to the definitive diagnosis of ADM, other causes of abdominal pain must first be ruled out [1]. Treatment for asymptomatic cases has not yet been determined. Although segmental and diffuse type of ADM consider prophylactic cholecystectomy, cholecystectomy cannot be recommended for a definitive diagnosis of asymptomatic fundal type of ADM. Considering the association between GB stones and chronic inflammation in patients with ADM, radiological follow-up can be recommended for cases with fundal type ADM without GB stones. For ADM with GB stones, particularly the combined type, advances of chronic inflammation should be considered. In addition, cholecystectomy cannot be recommended for all cases of fundal type ADM if not symptomatic, but the segmental and diffuse types of ADM consider prophylactic cholecystectomy.

The presence of intramural cysts is highly specific for the diagnosis of ADM [19]; however, intramural cysts have also been identified in xanthogranulomatous cholecystitis and mucin-producing GB carcinoma [20]. Although a definite diagnosis of ADM helps to exclude the possibility of gallbladder carcinoma, dysplastic changes and even carcinoma may arise from adenomyomatous epithelium [21, 22]. These consequences seem to be related to the presence of GB stones and chronic inflammation [14]. As ADM with chronic inflammation is benign, the clinical significance of this disease is not as great as that of GB carcinoma. Chronic inflammation combined with or without ADM is a common disease involving GB and may be hard to distinguish because thickening of the GB wall is nonspecific [23, 24]. Efforts to differentiate GB wall thickening have been made using various imaging modalities including ultrasonography, CT, and MRI [5, 25–29]. ADM with chronic inflammation is sometimes hard to distinguish from other GB disease such as ADM without chronic inflammation, xanthogranulomatous cholecystitis, and GB carcinoma. In contrast, ADM without GB stones exhibits chronic inflammation less frequently than ADM with GB stones and therefore has a lower possibility of dysplastic change or GB carcinoma.

Our study had some limitations. First, this was a retrospective analysis of a small case series. The number of

subjects was inadequate to draw generalized conclusions. A larger subject population is therefore needed. In addition, potential selection bias might have been present toward non-cholecystectomized patients because we recruited patients with surgically confirmed ADM. Second, MRI was performed without enhancement; enhancement studies were only performed in CT. Third, the type of GB wall-thickening was classified as a fundal type and a combined type. Although the segmental type of ADM has a higher risk of developing into GB cancer, the combined type of ADM, which includes the segmental and diffuse types, was used for accurate and simple assessment.

In conclusion, among the radiological findings of ADM, the presence of stones was independently associated with chronic inflammation in patients with ADM.

Compliance with ethical standards

Conflict of interest The authors declare that they have no competing interest.

References

1. Colquhoun J. Adenomyomatosis of the gall-bladder (intramural diverticulosis). Br J Radiol. 1961;34:101–12.
2. Williams I, Slavin G, Cox A, Simpson P, de Lacey G. Diverticular disease (adenomyomatosis) of the gallbladder: a radiological-pathological survey. Br J Radiol. 1986;59:29–34.
3. Golse N, Lewin M, Rode A, Sebagh M, Mabrut JY. Gallbladder adenomyomatosis: diagnosis and management. J Visc Surg. 2017;154:345–53.
4. Gerard PS, Berman D, Zafaranloo S. CT and ultrasound of gallbladder adenomyomatosis mimicking carcinoma. J Comput Assist Tomogr. 1990;14:490–1.
5. Ching BH, Yeh BM, Westphalen AC, Joe BN, Qayyum A, Coakley FV. CT differentiation of adenomyomatosis and gallbladder cancer. Am J Roentgenol. 2007;189:62–6.
6. Yoon JH, Cha SS, Han SS, Lee SJ, Kang MS. Gallbladder adenomyomatosis: imaging findings. Abdom Imaging. 2006;31:555–63.
7. Nabatame N, Shirai Y, Nishimura A, Yokoyama N, Wakai T, Hatakeyama K. High risk of gallbladder carcinoma in elderly patients with segmental adenomyomatosis of the gallbladder. J Exp Clin Cancer Res. 2004;23:593–8.
8. Cariati A, Cetta F. Rokitansky–Aschoff sinuses of the gallbladder are associated with black pigment gallstone formation: a scanning electron microscopy study. Ultrastruct Pathol. 2003;27:265–70.
9. Nishimura A, Shirai Y, Hatakeyama K. Segmental adenomyomatosis of the gallbladder predisposes to cholecystolithiasis. J Hepatobiliary Pancreat Surg. 2004;11:342–7.
10. Ootani T, Shirai Y, Tsukada K, Muto T. Relationship between gallbladder carcinoma and the segmental type of adenomyomatosisof the gallbladder. Cancer. 1992;69:2647–52.
11. Ash-Miles J, Roach H, Virjee J, Callaway M. More than just stones: a pictorial review of common and less common gallbladder pathologies. Curr Probl Diagn Radiol. 2008;37:189–202.
12. Tanno S, Obara T, Maguchi H, Fujii T, Mizukami Y, Shudo R, et al. Association between anomalous pancreaticobiliary ductal union and adenomyomatosis of the gall-bladder. J Gastroenterol Hepatol. 1998;13:175–80.
13. Chang LY, Wang HP, Wu MS, Huang HT, Wang HH, Lin CC, et al. Anomalous pancreaticobiliary ductal union—an etiologic association of gallbladder cancer and adenomyomatosis. Hepatogastroenterology. 1998;45:2016–9.
14. Khan SA, Thomas HC, Davidson BR, Taylor-Robinson SD. Cholangiocarcinoma. Lancet. 2005;366:1303–14.
15. Lin SH, Chang FY, Yang YS, Jin JS, Chen TW. Rare gallbladder adenomyomatosis presenting as atypical cholecystitis: case report. BMC Gastroenterol. 2011;11:106.
16. Boscak AR, Al-Hawary M, Ramsburgh SR. Best cases from the AFIP: adenomyomatosis of the gallbladder. Radiographics. 2006;26:941–6.
17. Kim BS, Oh JY, Nam KJ, Cho JH, Kwon HJ, Yoon SK, et al. Focal thickening at the fundus of the gallbladder: computed tomography differentiation of fundal type adenomyomatosis and localized chronic cholecystitis. Gut Liver. 2014;8:219–23.
18. Lalović N, Cvijanović R, Vladicić ND, Marić R, Jokanović D, Skipina DB. Adenomyomatosis of the gallbladder—case report. Med Pregl. 2011;64:323–6.
19. Catalano OA, Sahani DV, Kalva SP, Cushing MS, Hahn PF, Brown JJ, et al. MR imaging of the gallbladder: a pictorial essay. Radiographics. 2008;28:135–55.
20. Yoshimitsu K, Irie H, Aibe H, Tajima T, Nishie A, Asayama Y, et al. Well-differentiated adenocarcinoma of the gallbladder with intratumoral cystic components due to abundant mucin production: a mimicker of adenomyomatosis. Eur Radiol. 2005;15:229–33.
21. Levy AD, Murakata LA, Abbott RM, Rohrmann CA Jr. From the archives of the AFIP. Benign tumors and tumorlike lesions of the gallbladder and extrahepatic bile ducts: radiologic-pathologic correlation. RadioGraphics. 2002;22:387–413.
22. Haradome H, Ichikawa T, Sou H, Yoshikawa T, Nakamura A, Araki T, et al. The pearl necklace sign: an imaging sign of adenomyomatosis of the gallbladder at MR cholangiopancreatography. Radiology. 2003;227:80–8.
23. Shlaer WJ, Leopold GR, Scheible FW. Sonography of the thickened gallbladder wall: a nonspecific finding. Am J Roentgenol. 1981;136:337–9.
24. Teefey SA, Baron RL, Bigler SA. Sonography of the gallbladder: significance of striated (layered) thickening of the gallbladder wall. Am J Roentgenol. 1991;156:945–7.
25. Bang SH, Lee JY, Woo H, Joo I, Lee ES, Han JK, et al. Differentiating between adenomyomatosis and gallbladder cancer: revisiting a comparative study of high-resolution ultrasound, multidetector CT, and MR imaging. Korean J Radiol. 2014;15:226–34.
26. Kim SJ, Lee JM, Lee JY, Kim SH, Han JK, Choi BI, et al. Analysis of enhancement pattern of flat gallbladder wall thickening on MDCT to differentiate gallbladder cancer from cholecystitis. Am J Roentgenol. 2008;191:765–71.
27. Jung SE, Lee JM, Lee K, Rha SE, Choi BG, Kim EK, et al. Gallbladder wall thickening: MR imaging and pathologic correlation with emphasis on layered pattern. Eur Radiol. 2005;15:694–701.
28. Yun EJ, Cho SG, Park S, Park SW, Kim WH, Kim HJ, et al. Gallbladder carcinoma and chronic cholecystitis: differentiation with two-phase spiral CT. Abdom Imaging. 2004;29:102–8.
29. Smathers RL, Lee JK, Heiken JP. Differentiation of complicated cholecystitis from gallbladder carcinoma by computed tomography. Am J Roentgenol. 1984;143:255–9.